Electrophysiological and Morphological Characterization of Neurons Within Neocortical Ectopias

LISA A. GABEL AND JOSEPH J. LoTURCO
Department of Physiology and Neurobiology, University of Connecticut, Storrs, Connecticut 06269

Received 23 August 2000; accepted in final form 24 October 2000

Gabel, Lisa A. and Joseph J. LoTurco. Electrophysiological and morphological characterization of neurons within neocortical ectopias. *J Neurophysiol* 85: 495–505, 2001. Focal developmental abnormalities in neocortex, including ectopic collections of neurons in layer I (ectopias), have been associated with behavioral and neurological deficits. In this study, we used infrared differential interference contrast microscopy and whole cell patch-clamp to complete the first characterization of neurons within and surrounding neocortical ectopias. Current-clamp recordings revealed that neurons within ectopias display multiple types of action potential firing patterns, and biocytin labeling indicated that ~20% of the cells in neocortical ectopias can be classified as nonpyramidal cells and the rest as atypically oriented pyramidal cells. All cells had spontaneous excitatory (glutamatergic) and inhibitory (GABAergic) postsynaptic currents. Exhibitory postsynaptic currents consisted of both *N*-methyl-D-aspartate (NMDA) receptor-mediated and AMPA/kainate (A/K) receptor-mediated currents. The NMDA receptor-mediated component had decay time constants of 15.35 ± 2.2 (SE) ms, while the A/K component had faster decay kinetics of 7.6 ± 1.7 ms at −20 mV. $GABA_A$ receptor-mediated synaptic currents in ectopic cells reversed at potentials near the Cl^- equilibrium potential and had decay kinetics of 16.65 ± 1.3 ms at 0 mV. Furthermore we show that cells within ectopias receive direct excitatory and inhibitory input from adjacent normatopic cortex and can display a form of epileptiform activity.

INTRODUCTION

Focal neocortical malformations, including focal cortical dysplasias, microgyrias, nodular heterotopias, and molecular layer ectopias, have been associated with several neurological disorders (Arnold et al. 1991; Battaglia et al. 1997; Galaburda et al. 1985; Hannan et al. 1999; Humphreys et al. 1990; Lombroso 2000; Palmini et al. 1991a,b; Trottier et al. 1994). To better understand the role these malformations play in neurological malfunction, studies must be directed at understanding the cellular physiology of cells within and surrounding these malformations. In the past several years, animal models of several types of focal cortical malformations have been developed, and these models display pathologies similar to the human conditions. For example, microgyria and double cortex in rats have been shown to be associated with epileptiform activity in vitro and in vivo (Chen et al. 2000; Jacobs et al. 1996, 1999; Lee et al. 1997; Luhmann et al. 1998; Prince and Jacobs 1998; Prince et al. 1997).

Ectopias, clusters of misplaced cells in layer I of the neocortex, have been associated in humans with developmental dyslexia (Galaburda et al. 1985) and psychomotor retardation (Caviness et al. 1978). In brains of dyslexics, as many as 30–140 individual ectopias measuring 700–1,000 μm in diameter, which often extend into and disrupt the laminar pattern in cortical layers 2/3, were identified (Galaburda et al. 1985; Kaufmann and Galaburda 1989). The formation of ectopias appears to occur as a result of disrupted migration caused by either abnormal interactions between migrating neuroblasts and radial glial fibers (Caviness et al. 1978) and/or disruptions in the pia and layer 1 (Caviness et al. 1978; McBride and Kemper 1982).

Ectopias virtually identical to those described in humans have been found in three strains of autoimmune mice: NZB/BlNJ, BXSB/MPJ, and NXSM-D/Ei. Ectopias in these animals typically contain more than 50 cells, are located in either somatosensory or frontal/motor cortices, and are present in the brains of 40–85% of mice (Boehm et al. 1996; Denenberg et al. 1991; Sherman et al. 1990, 1994). Although the majority of mice with ectopias have only one ectopia, a small percentage have multiple ectopias (Boehm et al. 1996; Denenberg et al. 1991; Sherman et al. 1990). Behaviorally, mice with neocortical ectopias are impaired in certain learning tasks, such as spatial and nonspatial working memory (Balogh et al. 1998; Boehm et al. 1996; Denenberg et al. 1991; Schrott et al. 1993; Spencer et al. 1986), and in processing rapid auditory stimuli (Clark et al. 2000; Frenkel et al. 2000).

It remains unclear how ectopias are mechanistically linked to deficits in either humans or animal models. While altered local cortical and cortico-thalamic connections have been associated with ectopias (Jenner et al. 2000), the cellular physiology of cells within ectopias has yet to be described. In this study we have used whole cell patch-clamp techniques to characterize the physiological properties of cells within neocortical ectopias in NZB/BlNJ and NXSM-D/Ei mice. This paper provides evidence that layer I ectopias contain neurons with diverse cellular physiologies and morphologies, contain both GABAergic and glutamatergic synapses, receive direct inhibitory and excitatory connections from surrounding normatopic cortex, and, in some cases, can display epileptiform activity.

Address for reprint requests: J. J. LoTurco, 3107 Horsebarn Hill Rd., U-156, Dept. of Physiology and Neurobiology, University of Connecticut, Storrs, CT 06269 (E-mail: loturco@oracle.pnb.uconn.edu).

The costs of publication of this article were defrayed in part by the payment of page charges. The article must therefore be hereby marked "*advertisement*" in accordance with 18 U.S.C. Section 1734 solely to indicate this fact.

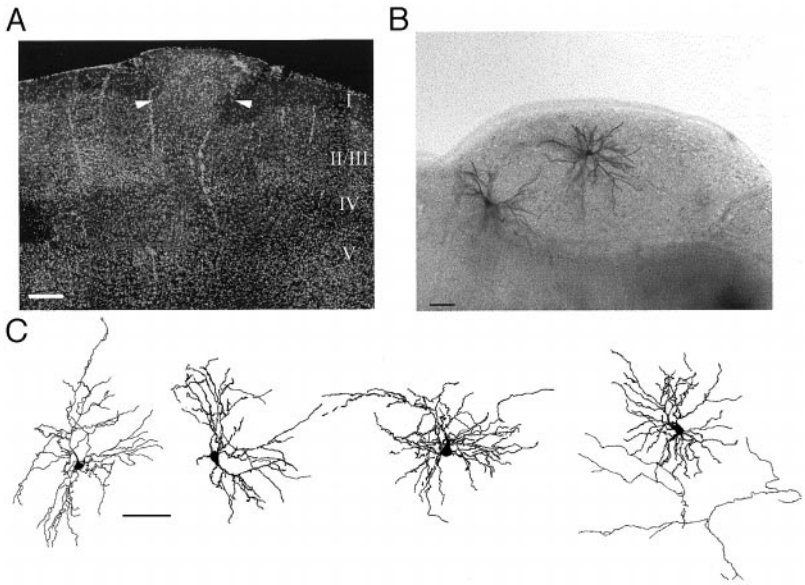

FIG. 1. Neocortical ectopias and constituent neurons located in the somatosensory cortex of adult NXSM-D/Ei and NZB/BlNJ mice. *A*: 50-μm-thick coronal section stained with 4,6-diamino-2-phenylindole (DAPI) shows an ectopic collection of neurons in layer I of the neocortex. *B*: 300-μm-thick coronal section showing 2 ectopic neurons that were intracellularly filled with biocytin during whole cell patch-clamp recording. *C*: camera lucida drawings of biocytin-filled cells within ectopias. Cells are oriented with the pial surface at the *top* of the figure. Scale bar = 50 μm.

METHODS

Whole cell recordings were made from neurons within and surrounding layer I neocortical ectopias. For the purposes of this study, an ectopia is defined as a large, cluster of misplaced cells in layer I of the neocortex. New Zealand black (NZB/BlNJ) and the recombinant in-bred NXSM-D/Ei mice, derived from a cross between NZB/BlNJ and SM/J mouse strains (Eicher and Lee 1990), both spontaneously develop large single-layer I ectopias located primarily in somatosensory cortices (Denenberg et al. 1991; Sherman et al. 1987). Based on the similarity in both location and size of the ectopias, the data have been collapsed across these two strains of mice.

Preparation of brain slices

Adult male and female NXSM-D/Ei and NZB/BlNJ mice (30–388 days postnatal) were deeply anesthetized with halothane and decapitated. Following decapitation, the brains were removed rapidly from the skull and immersed in an ice-cold, oxygenated sucrose-artificial cerebrospinal fluid (aCSF) solution containing (in mM) 124.0 sucrose, 5.0 KCl, 2.0 $MgCl_2$, 1.23 NaH_2PO_4 ($2 \cdot H_2O$), 23.8 $NaHCO_3$, and 2.0 $CaCl_2$; pH = 7.4. The brains were blocked, and 300-μm-thick coronal serial sections were cut using a Vibroslice (Campden Instruments, London, UK). Slices were transferred to a petri dish containing ice-cold, oxygenated aCSF and examined with oblique illumination under a dissecting microscope to identify slices containing ectopias (Fig. 1, *A* and *B*). aCSF contained (in mM) 124.0 NaCl, 5.0 KCl, 2.0 $MgCl_2$, 1.23 NaH_2PO_4 ($2 \cdot H_2O$), 23.8 $NaHCO_3$, and 2.0 $CaCl_2$; pH = 7.2, osmolarity = 300 ± 5 mOsm/l. Slices selected for recording were affixed to 18-mm circular microscope cover slips (Fisher Scientific, Pittsburgh, PA) with plasma/thrombin clots. Slices were maintained at room temperature (20–22°C) in aCSF for ≥1 h in an oxygenated holding chamber before recording began. Prior to whole cell recording, the 18-mm circular microscope cover slips containing slices were mounted onto the stage of a Nikon Eclipse 400 microscope. Recordings were performed at either room temperature (20–22°C) or 34–35°C.

Whole cell recordings

Whole cell recordings were made from cells within neocortical ectopias in somatosensory cortex. Slices were visualized, and neurons within ectopias were targeted using infrared differential interference contrast (IR-DIC) microscopy. Electrodes were pulled from capillary tubing (Garner Glass N51A, Garner Glass, Claremont, CA) using a Narishige multi-step electrode puller (Model PP-830) and had resistances of ~10 MΩ. The intracellular solution, used for voltage-clamp recordings, contained (in mM) 120.0 cesium gluconate, 10.0 ethylene glycol-bis (β-aminoethyl ether)-*N, N,N′,N′*-tetraacetic acid, 10.0 HEPES, 1.0 CsCl, and 1.0 $MgCl_2$; the pH was adjusted to 7.4 ± 0.05 with HCl 5.0 N and osmolarity was adjusted to 270 ± 5 mOsm/l. The intracellular solution used for current-clamp recordings contained (in mM) 120.0 potassium gluconate, 10.0 HEPES, 1.0 KCl, and 1.0 $MgCl_2$; the pH was adjusted to 7.4 ± 0.05 with HCl 5.0 N and osmolarity was adjusted to 270 ± 5 mOsm/l. In some experiments, pharmacological agents were used to selectively isolate the individual synaptic responses. Picrotoxin (PTX) and bicuculline methiodide (BMI) were purchased from Sigma Chemicals (St. Louis, MO). d-(−)-2-amino-5-phosphonovaleric acid (d-AP5) and 6,7-dinitroquinoxaline-2,3-dione (DNQX) were purchased from Tocris Cookson (St. Louis, MO).

Voltage- and current-clamp recordings were made using an Axon Instruments 200B amplifier (Axon Instruments, Foster City, CA) and low-pass filtered at 1 kHz. Currents were digitally sampled at 10 kHz and monitored with pCLAMP 7.0 software (Axon Instruments) running on a PC pentium computer.

A bipolar stimulating electrode was placed in sites adjacent and below ectopias (~400 μm), using pulses of 100 μs and 50–400 μA, unless otherwise noted. To examine the synaptic properties of ectopias, both paired-pulse and potentiation protocols were used. Maximal stimulation was determined by applying increasing stimulation using pulses of 100 μs and between 50 μA to 1 mA at 15-s intervals. Paired pulses, at 50–75% maximal stimulation, were recorded at interstimulus intervals of 50, 100, 200, 300, 400, 500, 600, 700, and 800 ms. Potentiation was induced using 7 cycles of a 50 Hz stimuli (80 ms) applied at 0.1 Hz while the cells were depolarized to about −20 mV, after a baseline level of activity was recorded for ~10 min. Potentiation was defined as a ≥20% increase in postsynaptic potential (PSP) amplitude immediately following tetanization, which was sustained for ≥10 min.

Data analysis

Spontaneous and evoked postsynaptic currents (PSCs) were detected and measured using Mini Analysis 5.0 software (Synaptosoft), which identifies spontaneous currents on the basis of several criteria, including threshold, amplitude, decay, and rise time properties of each event. Although the program is designed to automatically detect

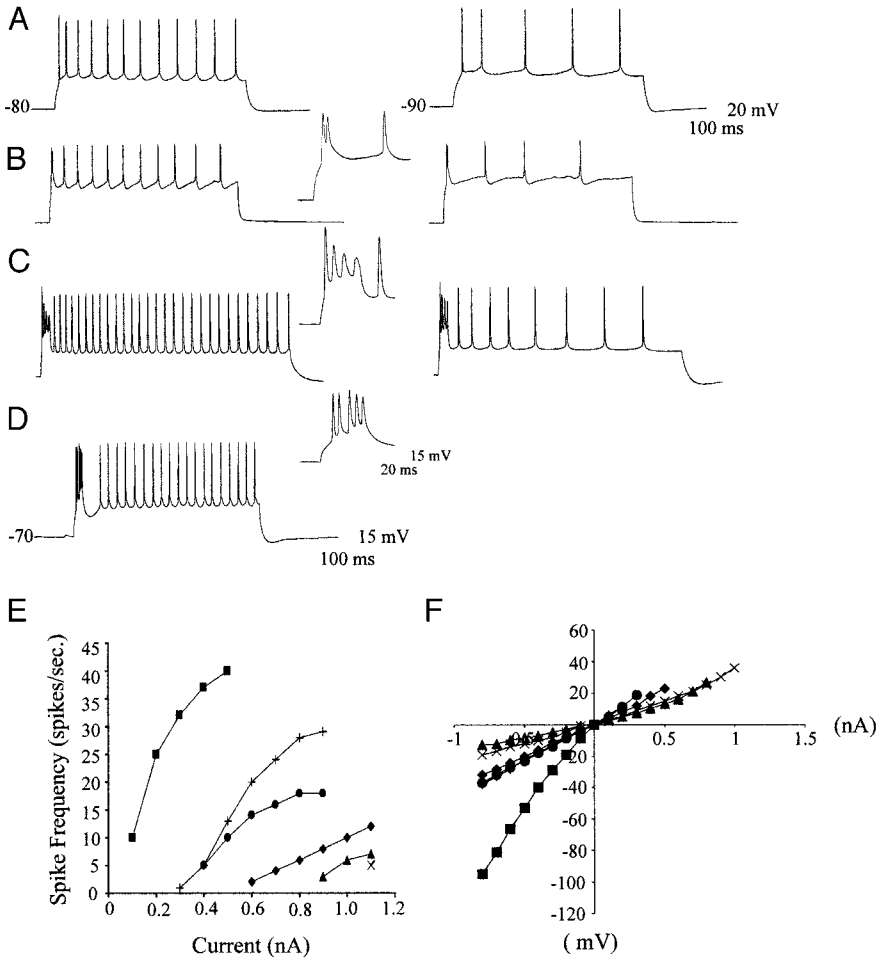

FIG. 2. Neurons within ectopias exhibit a variety of different firing patterns. *A–C*: room temperature, current-clamp recordings at membrane potentials of −80 and −90 mV with current injections of 0.6, 1.1, and 0.2 nA, respectively. *A*: regular spiking. *B* and *C*: burst discharge accommodating action potential properties. *D*: burst discharge non-accommodating action potential recorded at 34–35°C. *B–D, insets*: expanded traces of the initial burst discharge. *E*: a plot of the spike frequencies vs. current injection for 6 cells recorded at room temperature. Spike frequencies were calculated by counting the total number of action potentials during a 900-ms step. *F*: a plot of the subthreshold current-voltage relationship for 6 cells recorded at room temperature.

events based on these criteria, each event was manually selected based on rise time and decay properties. In some cases, PSPs were identified and analyzed using Clampfit 8 software (Axon Instruments). Kinetic analysis of the PSCs were performed by fitting the decaying phase of the PSCs with a single-exponential function. To increase the signal to noise ratio of traces that had peak amplitudes that were just above noise, the traces were filtered at 1 kHz and then analyzed based on rise-time and decay properties. All data throughout this report are expressed as means ± SE unless indicated otherwise.

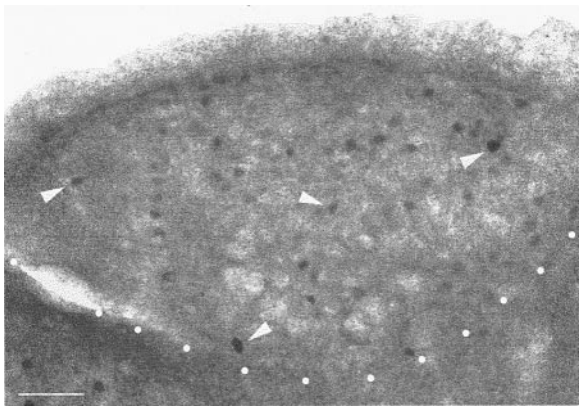

FIG. 3. Some cells within ectopias are immunopositive for GABA. Neurons within ectopias in 50-μm free-floating sections immunoreacted with anti-GABA antibodies (arrowheads), demonstrating that GABAergic interneurons are present within ectopias. Filled circles outline the ectopia border. Scale bar = 50 μm.

Histological procedures

In all recordings, biocytin (Sigma), ~1–2%, was included in the internal pipette solution. Following electrophysiological recording, the tissue was fixed in 4% paraformaldehyde for ≥24 h at 4°C. The tissue was rinsed in phosphate buffered saline (PBS) prior to histochemical analysis. Sections (300 μm) were treated in 0.5% H_2O_2 in PBS for 20–30 min at room temperature (RT) to eliminate endogenous peroxidase activity. Sections were then permeabilized and blocked with 0.2% Triton X-100 and 1% normal goat serum (NGS) in PBS overnight at 4°C. Tissue was washed in PBS and then incubated with VECTISTAIN elite ABC reagent (Vector Laboratories) overnight at 4°C. The tissue was washed in PBS and then reacted with diaminobenzidine tetrahydrochloride substrate (DAB; Vector Laboratories) for 10–15 min at RT. Sections were rinsed in PBS and cleared with 100% glycerol for viewing with a Nikon Eclipse E-400 microscope. Figure 1, *B* and *C*, provides examples of intracellularly labeled cells, as well as camera lucida reconstructions of cells located within neocortical ectopias of adult NXSM-D/Ei and NZB/BlNJ mice. In some cases 1:2,000 dilution of 4,6-diamino-2-phenylindole (DAPI) in PBS was applied for 5 min to visualize the ectopia as well as the disruption the ectopia causes to the underlying cortical layers (Fig. 1*A*).

Immunocytochemistry

Mice were transcardially perfused with PBS followed by 4% paraformaldehyde. Brains were postfixed overnight at 4°C, blocked in 1.5–1.9% agar, and sectioned in the coronal plane on a vibratome. Free-floating sections (50 μm) were then collected into different wells

for immunocytochemistry. Fixed sections were first washed with PBS and then preblocked in 5% NGS and 0.2% Triton X-100 for 1 h. Sections were incubated with rabbit anti-GABA (1:10,000) in 0.1% Triton X-100, 2.5% NGS, and PBS at 4°C for 40 h. The tissue was then rinsed several times with 2.5% NGS in PBS and then incubated in biotinylated goat-anti-rabbit (1:200) secondary antibody for 2 h at RT. Sections were rinsed several times with PBS and incubated for 1 h in an avidin and biotinylated horseradish peroxidase mixture. The tissue was rinsed in PBS and then reacted with 0.05% diaminobenzidine in the presence of 0.0015% H_2O_2, and 0.04% nickel chloride. Sections were collected onto gelatin-coated slides, dried for several hours, and coverslipped with Cytoseal.

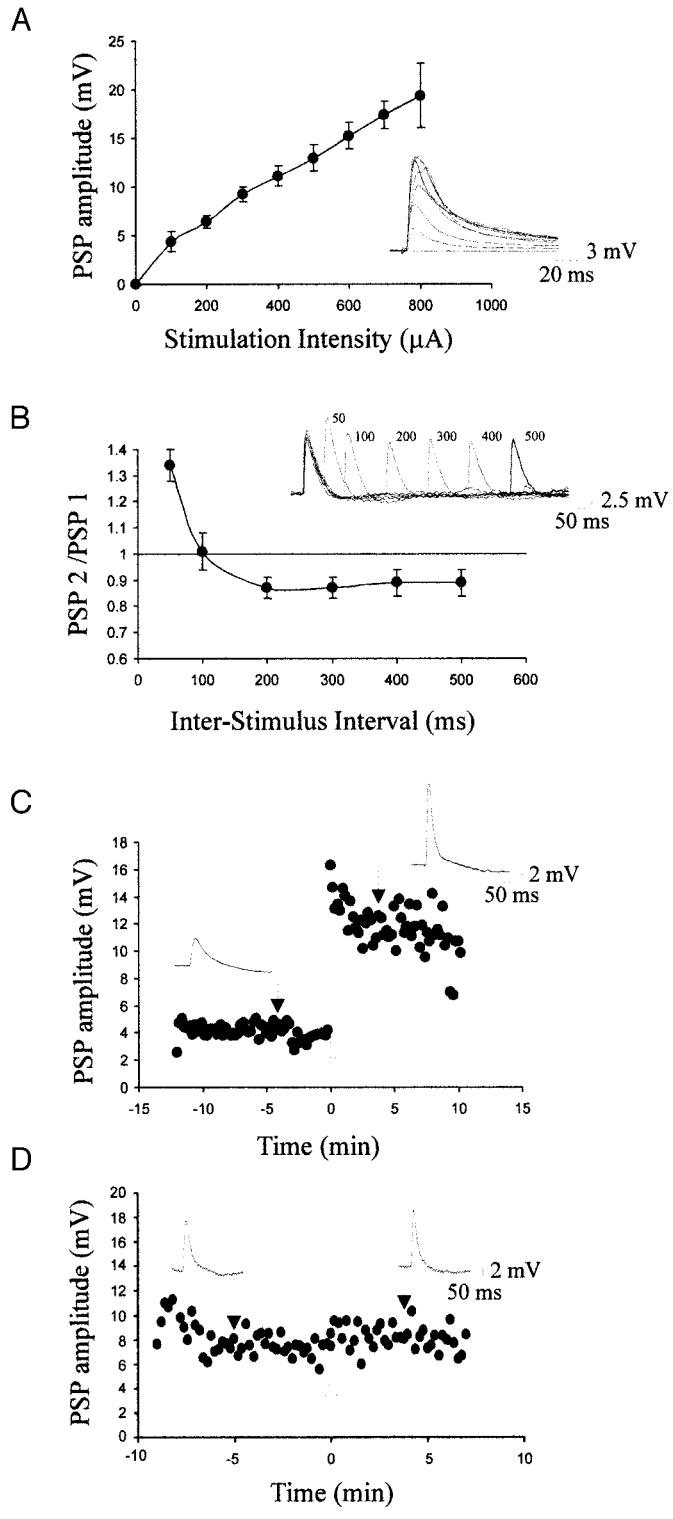

RESULTS

Ectopias contain diverse cell types

Layer I ectopias visible in slices examined under a dissecting microscope (Fig. 1, *A* and *B*) were present in 43% (30/70) of all male and 41% (11/27) of all female NXSM-D/Ei (10/17 female; 27/50 male) and NZB/BlNJ mice (1/10 female; 3/20 male). On average there was only one ectopia present per animal, with a preference of occurrence within the somatosensory cortex. In one brain we identified two ectopias located adjacent to each other within the somatosensory cortex. Whole cell recordings were made from a total of 164 cells within and surrounding these ectopias. Cells within ectopias had resting membrane potentials of -63.5 ± 0.7 mV, input resistances of 53.1 ± 10.0 MΩ, and fired multiple action potentials to depolarizing stimuli.

Cells in normatopic neocortex exhibit diverse action potential patterns associated with different neuronal cell types. These types include regular spiking cells, typically associated with pyramidal cells, bursting cells, characteristic of some layer 5 cells, and a variety of fast-spiking interneuron types (Agmon and Connors 1989; Cauli et al. 1997; Gupta et al. 2000; Kawaguchi 1993; Kawaguchi and Kubota 1993; McCormick et al. 1985). Similarly cells in ectopias exhibited a variety of different firing patterns and accommodation rates. The firing patterns included regular spiking (85%; Fig. 2*A*), burst-discharge accommodating (10%; Fig. 2, *B* and *C*), and burst-discharge non-accommodating neurons (5%; Fig. 2*D*). A plot of the spike frequency versus depolarizing current injection for six representative cells in ectopias, recorded at RT, further demonstrates the variety of firing properties exhibited by neurons within ectopias (Fig. 2*E*). Layer I ectopias, therefore, contain neurons with diverse cellular physiologies.

Consistent with the electrophysiologies, the morphologies of ectopic cells, determined by intracellular labeling with biocytin, were diverse. Figure 1*C* shows several examples of camera lucida reconstructions of the cells located inside ectopias. Neurons within ectopias can be identified as either atypically oriented spiny pyramidal cells (Figs. 1*C* and 8*A*) or aspiny and sparsely spiny nonpyramidal cells. The pyramidal to nonpyramidal cell ratio was ~5:1, and the presence of significant numbers of nonpyramidal cells was further confirmed by immunocytochemical labeling for γ-aminobutyric acid (GABA; Fig. 3).

FIG. 4. Properties of postsynaptic potentials within ectopias. *A*: a plot of the average postsynaptic potential (PSP) amplitude vs. stimulation intensity ($n = 23$). *Inset*: an example of saturation of PSP amplitude to 600-μA stimulation. *B*: a plot of the average PSP 2: PSP 1 ratio vs. inter-stimulus interval (ISI). Paired-pulse facilitation is evident in response to short inter-spike intervals (ISIs) of 50 ms and paired-pulse depression due to ISIs of ≥200 ms ($n = 7$). *Inset*: an example of responses to the paired-pulse protocol from 1 cell. *C*: a plot of the PSP amplitude pre- and post-tetanus. A tetanic stimulus was applied at *time 0* (△). *Inset traces* show examples of the PSP both pre- and post-tetanus (↓). Potentiation occurred following tetanic stimulation. *D*: a plot of the PSP amplitude pre- and posttetanus. A tetanic stimuli was applied at *time 0* (△). *Inset traces* show examples of the PSP both pre- and post-tetanus (↓). Potentiation did not occur following tetanic stimulation.

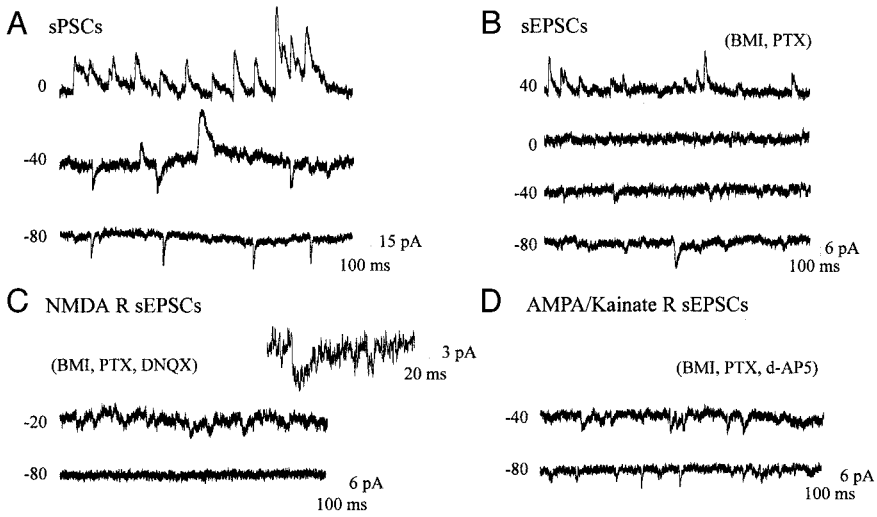

FIG. 5. Isolation of spontaneous excitatory postsynaptic events. *A*: spontaneous postsynaptic currents were recorded at membrane potentials between 0 and −80 mV. The responses at −40 mV reveal both inward and outward postsynaptic currents. *B*: spontaneous excitatory postsyaptic currents (sEPSCs) recorded in the presence of picrotoxin (PTX, 10 μM) and bicuculline methiodide (BMI, 10 μM). *C*: *N*-methyl-D-aspartate (NMDA)-mediated component of the sEPSC was recorded in the presence of 6,7-dinitroquinoxaline-2,3-dione (DNQX, 10 μM). Note the characteristic slow decay as well as the voltage-dependent block at −80 mV. *D*: the AMPA/kainate (A/K) sEPSCs were isolated with application of D-(−)-2-amino-5-phosphonovaleric acid (d-AP5, 50 μM) and do not show the voltage-dependent block of the NMDA receptor-mediated component.

Characterization of synaptic properties within ectopias

Extracellular stimulation of white matter beneath ectopias reliably produced excitatory PSPs (23/23, Fig. 4*A*) within ectopic neurons. Paired-pulse experiments showed that with short inter-stimulus intervals (ISIs; 50 ms) paired-pulse facilitation was evident (PSP2: PSP1 ratio of 1.34 ± 0.06), while ISIs of 200 ms, or longer, produced a depression in the second PSP amplitude (Fig. 4*B*; $n = 7$). To examine the potential for plasticity at ectopia synapses, seven cycles of 50-Hz stimuli (80 ms) were applied at 0.1 Hz while the cells were depolarized to about −20 mV. Potentiation was defined as a 20% increase, or greater, in PSP amplitude immediately following tetanization, which was sustained for ≥10 min. Potentiation was elicited in one of four cells tested when the stimulating electrode was placed in layer IV of the neocortex (Fig. 4*C*), and zero of nine cells tested when the stimulating electrode was placed in the white matter (WM)/layer VI border (Fig. 4*D*).

TABLE 1. *Comparison of sPSCs*

Receptor	Vm, mV	Ectopic	Normatopic
A/K			
Amplitude, pA	−80	7.01 ± 0.81	9.72 ± 1.07
Decay, ms		4.53 ± 0.51	3.94 ± 0.61
Frequency, Hz		0.58 ± 0.20	0.82 ± 0.29
NMDA			
Amplitude, pA	−20	7.87 ± 1.09	9.29 ± 1.06
Decay, ms		11.76 ± 1.19	10.48 ± 1.12
Frequency, Hz		0.15 ± 0.04	0.13 ± 0.03
$GABA_A$			
Amplitude, pA	0	14.09 ± 1.54	13.89 ± 2.69
Decay, ms		16.45 ± 2.05	14.04 ± 0.71
Frequency, Hz		4.01 ± 0.92	4.29 ± 1.48

Values are means ± SE. There were no significant differences found between spontaneous postsynaptic currents (sPSCs) recorded within ectopias (Ectopic) and sPSCs recorded in layer II/III of the normatopic cortex (Normatopic). Excitatory PSCs were isolated using $GABA_A$ blockers, bicuculline methiodide (BMI, 10 μM) and picrotoxin (PTX, 10 μM). AMPA/kainate (A/K) receptor-mediated PSCs were isolated using d-(−)-2-amino-5-phosphonovaleric acid (d-AP5, 50 μM) and were blocked with DNQX (10 μM). GABA receptor mediated PSCs were isolated using d-AP5 (50 μM) and dinitroquinoxaline-2,3-dione (DNQX, 10 μM). All values are based on averages of ≥6 cells for each condition. Statistical analyses were performed using a single-factor ANOVA. All F values <1, except for the amplitude of A/K receptor-mediated events recorded at −80 mV, which had an F value of 3.77. All P values >0.05. NMDA, *N*-methyl-D-aspartate.

Glutamatergic and GABAergic synapses within ectopias

To determine the types of synapses formed on cells within ectopias, we characterized the spontaneous synaptic currents recorded from cells within ectopias. At holding potentials of −40 mV both inward and outward spontaneous synaptic currents were apparent, suggesting the presence of both excitatory and inhibitory synapses (16 of 16 cells) (Fig. 5*A*). $GABA_A$ receptor blockers BMI (10 μM) and PTX (10 μM) eliminated the population of synaptic currents that were outward at −40 mV (Fig. 5*B*). The remaining spontaneous synaptic currents reversed at approximately 0 mV and could be completely blocked by a combination of d-AP5 (50 μM) and DNQX (10 μM). Blockade of *N*-methyl-D-aspartate (NMDA) receptors alone with d-AP5 revealed AMPA/kainate (A/K) receptor-mediated synaptic events that were linearly related to membrane potential. Representative traces in Fig. 5 had peak amplitudes of 8.93 ± 0.69 pA, rapid decay time constants (7.6 ± 1.7 ms at −20 mV), and conductances of 4.5 ± 0.4 nS (Fig. 5*D*). In contrast, blockade of A/K receptors revealed NMDA receptor-mediated spontaneous synaptic events that showed voltage-dependent block at −80 mV (Fig. 5*C*), had peak amplitudes of 4.82 ± 0.34 pA, had decay time constants of 15.35 ± 2.2 ms, and had conductances of 2.4 ± 0.2 nS at −20 mV. Averages of all cells tested are presented in Table 1. In addition, the A/K receptor-mediated synaptic currents occurred at higher frequencies than NMDA receptor-mediated synaptic currents (at −20 mV: 0.3 events/s for A/K receptor-mediated currents, and 0.17 events/s for NMDA receptor-mediated currents).

To characterize the GABAergic synaptic currents, a cocktail of d-AP5 (50 μM) and DNQX (10 μM) was used to block glutamatergic events. The remaining events could be blocked by addition of PTX and BMI and are therefore mediated by $GABA_A$ receptors. Figure 6*A* shows the PSCs mediated by activation of $GABA_A$ receptors. These currents had reversal potentials of near the calculated Cl^- equilibrium potential of −65 mV (Fig. 6*B*), had peak amplitudes of 13.74 ± 1.162 pA, had decay time constants of 26.8 ± 3.1 ms at 0 mV (Fig. 6*C*), occurred at a mean frequency at 0 mV of 5.1 events/s, and had conductances of 0.23 ± 0.02 nS at 0 mV (Fig. 6*D*). Cells in ectopias, therefore, contain both GABAergic and glutamatergic synapses.

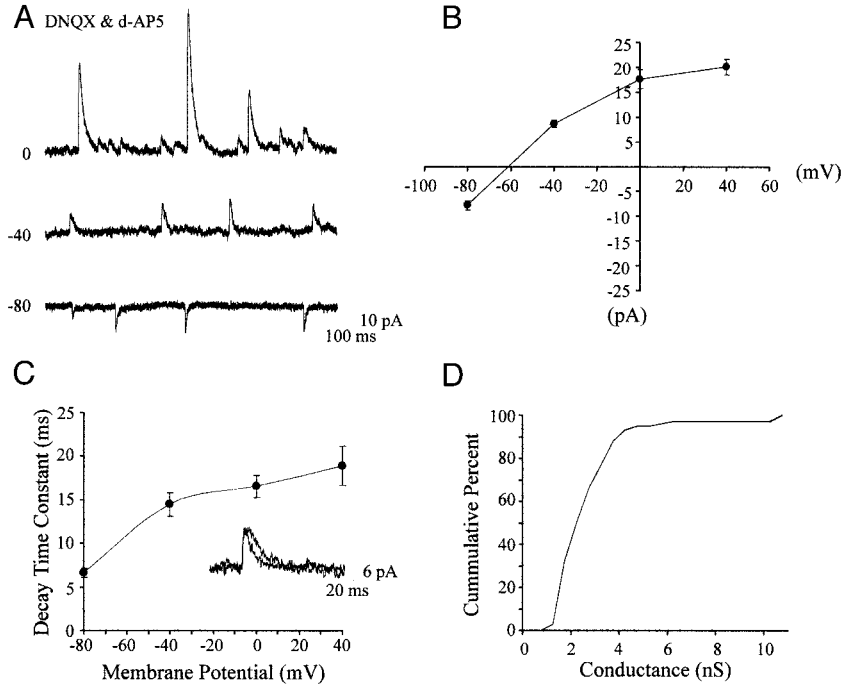

FIG. 6. Spontaneous inhibitory postsynaptic currents (sIPSCs) recorded in the presence of d-AP5 (50 μM) and DNQX (10 μM). *B*: an *I-V* plot of the average peak current amplitude vs. the holding potential reveals an E_{rev} near the calculated E_{Cl^-} of −65 mV. *C*: plot of the average decay time constant vs. membrane potential of the traces in *A* (0 mV, 16.65 ± 1.27 ms). *Inset*: normalized, expanded current traces from *A* at 40 and −80 mV. *D*: cummulative percent plot of the conductance of responses in *A*. The average conductance values at 0 mV were 2.5 ± 0.23 nS.

Ectopias receive direct excitatory inputs from normatopic cortex

To determine whether ectopias receive input from adjacent normatopic cortex, extracellular stimulation (0.1- to 0.2-ms, 50- to 400-μA current) was delivered to multiple adjacent sites in normatopic cortex. A bipolar stimulating electrode was placed in layer 2/3, ≤400 μm medial or lateral to the ectopia or ≤300 μm within the axon fascicles directly below the

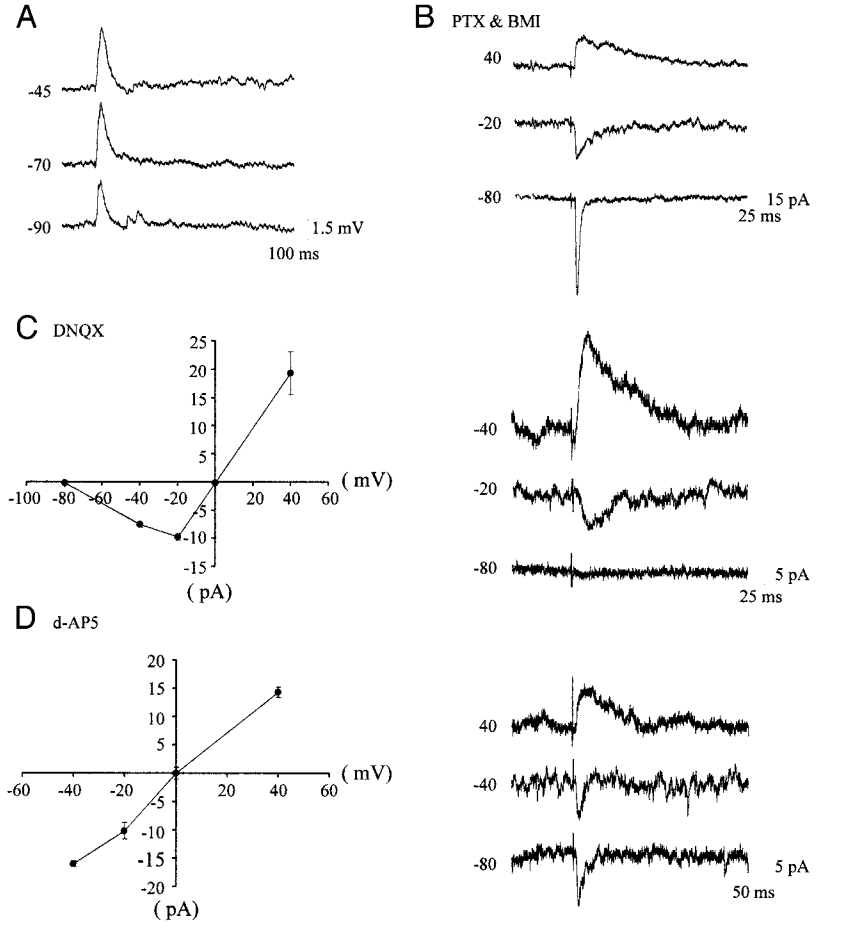

FIG. 7. Characterization of evoked excitatory postsynaptic events by stimulation of the surrounding cortex. *A*: evoked PSPs increase in amplitude with depolarization. PSP evoked by 50-μA stimulation. *B*: evoked EPSCs (eEPSCs) are recorded in the presence of PTX (10 μM) and BMI (10 μM). PSP evoked by 150-μA stimulation. *C*: a plot of the current-voltage relationship of NMDA receptor-mediated currents shown in *D*. *D*: the NMDA-mediated component of the eEPSC was isolated following application of DNQX (10 μM). PSP evoked by 200-μA stimulation. *E*: an *I-V* plot reveals a E_{rev} of ~0 mV as well as a linear current-voltage relationship. *F*: isolation of the A/K receptor-mediated component of the eEPSCs with the application of d-AP5 (50 μM). PSP evoked by 300-μA stimulation.

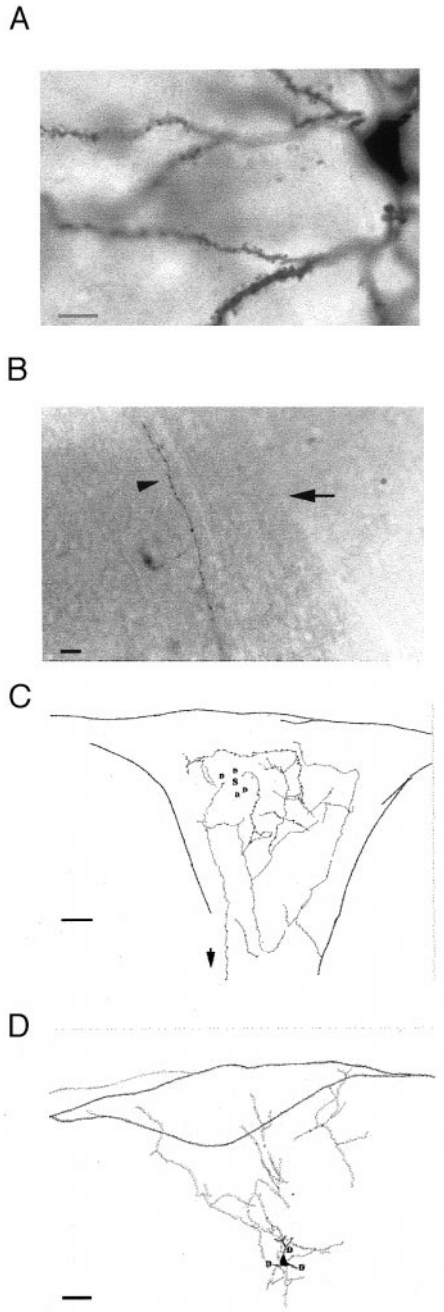

FIG. 8. Morphological properties of dendrites and axons within and around ectopias. *A*: high magnification of spines on the dendrites of an atypically oriented pyramidal cell. *B*: axon (▲) leaving an ectopia via axon fascicles (←). Scale bars for *A* and *B* = 10 μm. *C*: camera lucida reconstruction of the axon of a cell within an ectopia. The axon stays within the boundaries of the ectopia (darker lines), but projects down the axon fascicles which extend from the base of the ectopia. The soma and primary dendrite locations are indicated by "S" and "D," respectively. Scale bar = 100 μm. *D*: camera lucida reconstruction of an axon of a pyramidal cell outside an ectopia. The axon projects past the ectopia border (darker lines) demonstrating that pyramidal cells outside the ectopia can extend their axons into ectopias. Scale bars for *C* and *D* = 50 μm.

ectopia. The axon fascicles are the same as the "bundle of fibers" reported by Sherman et al. (1990). Excitatory postsynaptic potentials were consistently elicited on stimulation of all sites surrounding the ectopias (Fig. 7*A*; $n = 23$).

To further characterize the excitatory inputs, $GABA_A$ blockers (BMI and PTX) were applied to the bath solution (Fig. 7*B*). Evoked exhibitory postsynaptic currents (EPSCs) had a fast initial component and a late component that showed voltage-dependent block at −80 mV. The late component was isolated by addition of DNQX, and it had an average peak amplitude of 9.6 ± 0.6 at −20 mV, decay time constant of 20.5 ± 2.6 ms (Fig. 7*D*), and exhibited voltage-dependent block at −80 mV (Fig. 7*C*). The A/K receptor-mediated component was isolated by blocking NMDA receptors (d-AP5, 50 μM), and it reversed at 0 mV (Fig. 7*E*), had an average peak amplitude of 11.5 ± 0.5 pA at −20 mV, and had rapid decay time constants of 8.0 ± 1.4 ms at −20 mV (Fig. 7*F*). Antidromic responses were rarely observed (1/29; 3%) due to stimulation of the surrounding cortex. In addition, labeled pyramidal cells outside of ectopias were found to send axon collaterals into ectopias (Fig. 8*D*). Ectopias, therefore receive direct excitatory connections from surrounding normatopic cortex.

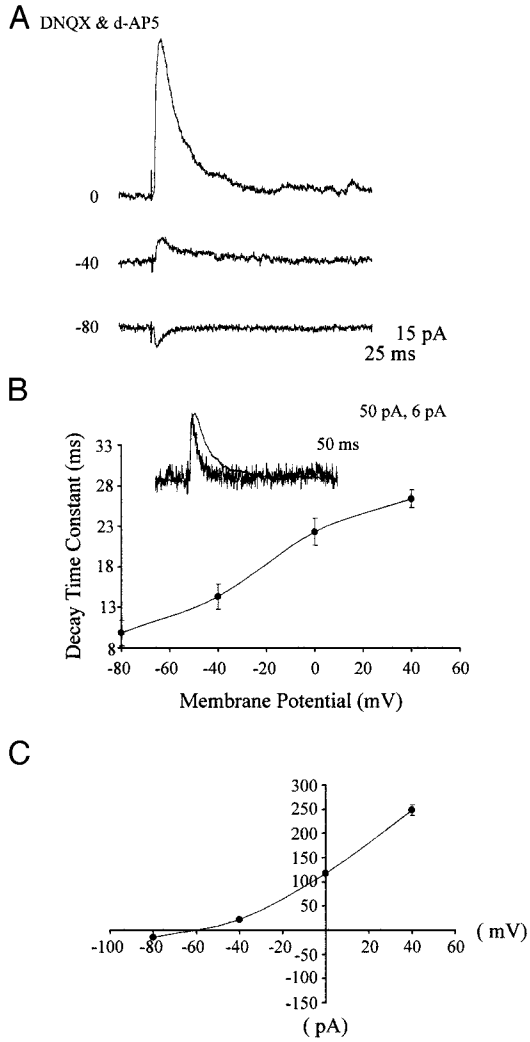

FIG. 9. Characterization of evoked inhibitory events by stimulation of the surrounding cortex. *A*: eIPSCs recorded in the presence of d-AP5 (50 μM) and DNQX (10 μM) at membrane potentials between 0 and −80 mV. PSP evoked by 200-μA stimulation. *B*: plot of the average decay time constants vs. membrane potential of the traces in *A* (0 mV, 22.3 ± 1.65 ms). *Inset*: normalized, expanded current traces from *A* at 0 and −80 mV. These currents can be fit with a single exponential function. *C*: an *I-V* plot of the average peak amplitude vs. holding potential reveals an E_{rev} near the calculated E_{Cl^-} of −65 mV.

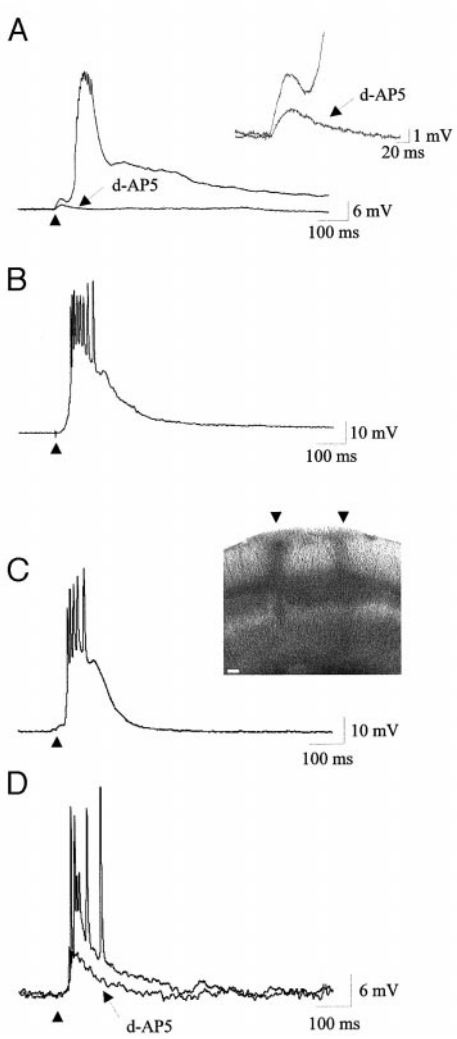

FIG. 10. Ectopic cells can display epileptiform activity. *A*: application of $GABA_A$ blockers, PTX (10 μM) and BMI (10 μM), at −80 mV reveals an epileptiform discharge that is blocked by application of d-AP5 (50 μM). Initial PSP evoked by 50-μA stimulation (▲). *B*: recordings made at 34–35°C show an decrease in latency of the epileptiform discharge produced after application of $GABA_A$ blockers, PTX (10 μM) and BMI (10 μM) at −80 mV. Initial PSP evoked by 100-μA stimulation (▲). *C* and *D*: recordings made at 34–35°C in a slice that contains 2 adjacent ectopias (*inset*). *C*: epileptiform-like discharge is produced within the medial ectopia following 120-μA stimulation (▲). *D*: epileptiform-like discharge is produced within the lateral ectopia following 110-μA stimulation (▲) and is reduced by application of d-AP5 (50 μM).

Ectopias receive direct inhibitory input from normatopic cortex

When all glutamatergic transmission was blocked with DNQX and d-AP5, monosynaptic GABAergic synaptic currents were reliably produced by extracellular stimulation (0.1- to 0.2-ms, 50- to 400-μA current) delivered to multiple adjacent sites in normatopic cortex (Fig. 9*A*). Bipolar stimulating electrode was placed in layer 2/3, ≤400 μm either medial or lateral to the ectopia or within the axon fascicles directly below the ectopia (≤300 μm). Similar to spontaneous GABAergic synaptic currents, the evoked inhibitory postsynaptic currents (eIPSCs) had reversal potentials of about −60 mV (Fig. 9*C*), had decay time constants of 22.3 ± 1.65 ms at 0 mV (Fig. 9*B*), and were sensitive to application of BMI and PTX (data not shown). Therefore ectopias receive both direct inhibitory and excitatory connections from surrounding normatopic cortex.

Epileptiform discharges in ectopias

In disinhibited slices (10 μM BMI and 10 μM PTX), low depolarizing stimulation (50 μA) of WM/layer VI border elicited late epileptiform discharges (latency, 104 ± 8.7 ms) in cells within ectopias (Fig. 10*A*). These large discharges within ectopias were of variable latency, 46.3–174.5 ms and were associated with a large post-discharge depolarization and multiple action potentials. As expected, the latency of epileptiform discharges were much faster on heating the slice to 34–35°C (latency 20.84 ± 1.98 ms; Fig. 10*B*). The epileptiform discharges could be blocked with d-AP5 (Fig. 10*A*).

In 23 cells recorded in slices with single ectopias at 35°C, we never observed epileptiform discharges without the addition of $GABA_A$ receptor blockers. Epileptiform discharges, however, could be elicited in the absence of $GABA_A$ blockers, in the only slice which contained two ectopias positioned adjacent to one another (Fig. 10*C*, *inset*). Extracellular stimulation (110–120 μA) of the WM/layer VI border initiated epileptiform discharges in two neurons recorded from both ectopias (Fig. 10, *C* and *D*). The discharges were of variable latency (9.9–58.9 ms; 25.57 ± 4.16), and could be blocked with d-AP5 (Fig. 10*D*). Therefore multiple ectopias appear to be necessary to create an epileptogenic cortical slice.

DISCUSSION

Our results demonstrate that ectopias contain neurons that have a variety of intrinsic firing patterns and morphologies, have both glutamatergic and GABAergic synapses, receive direct excitatory and inhibitory input from outside of the ectopia, and can show epileptiform bursts if slices are either disinhibited or contain two ectopias. These findings are discussed with respect to properties in normatopic neocortex and to properties of other forms of neocortical dysplasias.

Ectopias contain diverse cell types

Neurons within normatopic neocortex exhibit diverse forms of intrinsic firing patterns that are associated with different neuronal types. Spiny pyramidal cells have been classified based on their different patterns of regular and bursting action potential patterns (Agmon and Connors 1989; McCormick et al. 1985), and similarly nonpyramidal cells have been classified into a variety of types including irregular spiking, fast spiking (Cauli et al. 1997; Kawaguchi 1993; Kawaguchi and Kubota 1993), accommodating, non-accommodating, or stuttering (Gupta et al. 2000). While we did not observe cells in ectopias in all categories reported in the literature for neocortex, we did record from cells in ectopias that had properties of regular spiking pyramidal cells, burst-discharge accommodating, and burst-discharge non-accommodating nonpyramidal cells. Interestingly, we did not record from any cells that were classic "fast spiking cells." Nevertheless the morphologies and presence of GABA-positive cells in ectopias indicate that there are nonpyramidal interneurons within ectopias. Consistent with this, biocytin-filled cells within ectopias could be classified as either atypically oriented spiny pyramidal cells or sparsely

spiny and aspiny nonpyramidal cells. The ratio of pyramidal to nonpyramidal cells using these morphological criterion was 5:1, similar to the pyramidal to nonpyramidal cell ratio in normatopic cortex (Hendry et al. 1987; Parnavelas et al. 1977). The fact that no nonpyramidal cells in ectopias showed a classic fast-spiking non-accommodating pattern of activity could indicate that only a subset of interneuron types reside within ectopias or that the development of the physiology of interneurons within ectopias is altered.

Excitatory synapses within ectopias

The two main types of synapses made by neurons within normatopic cortex, excitatory glutamatergic synapses and GABAergic synapses, are both present on neurons within ectopias. Moreover similar to synapses described in normatopic cortex and hippocampus in rats and mice, cells within ectopias have glutamatergic synapses that are mediated by both A/K and NMDA receptor activation (Fleidervish et al. 1998; Hablitz and Sutor 1990; Hestrin 1993; Hestrin et al. 1990a,b; Konnerth et al. 1990; LoTurco et al. 1990; Sutor and Hablitz 1989). The A/K receptor-mediated synapses within ectopias have a linear current-voltage relationship, DNQX sensitivity, and rapid decay time constants similar to normatopic cortical and hippocampal neurons (Fleidervish et al. 1998; Hestrin 1993; Hestrin et al. 1990; LoTurco et al. 1990). NMDA receptor-mediated synapses within ectopias have nonlinear current-voltage relationships, d-AP5 sensitivity, and slow decay time constants similar to cortical and hippocampal neurons (Berretta and Jones 1996; Hablitz and Sutor 1990; Konnerth et al. 1990; LoTurco et al. 1990; Sutor and Hablitz 1989). Similarly recordings of supragranular cells in normatopic cortex in NXSM-D/Ei and NZB/BlNJ mice, which provide a more direct comparison of excitatory events, show that the amplitudes, decay time constants, and frequencies of A/K and NMDA receptor-mediated events recorded within ectopias were not significantly different from those recorded in normatopic layer II/III cells in NXSM-D/Ei and NZB/BlNJ mice (Table 1).

Inhibitory synapses within ectopias

$GABA_A$ receptor-mediated synaptic events within ectopias have similar properties to normatopic cortical cells. The present results indicate that $GABA_A$ receptor-mediated synaptic events within ectopias have similar peak amplitudes (range of 5–156 pA) to those reported for cortical cells of supragranular and infragranular layers (Ling and Bernardo 1999; Salin and Prince 1996). The decay kinetics of $GABA_A$ receptor-mediated synaptic events within ectopias (27 ms) are similar to those reported for cortical and hippocampal cells at similar recording temperatures (Galarreta and Hestrin 1997; Ropert et al. 1990; Zhou and Hablitz 1997), but as expected were significantly slower than spontaneous IPSCs (sIPSCs) recorded at higher temperatures (Ling and Bernardo 1999; Otis and Mody 1992; Otis et al. 1991; Salin and Prince 1996). Recordings of supragranular cells in normatopic cortex in NXSM-D/Ei and NZB/BlNJ mice show that the amplitudes, decay time constants, and frequencies of $GABA_A$-receptor-mediated events recorded within ectopias were not significantly different from those recorded in normatopic layer II/III cells in NXSM-D/Ei and NZB/BlNJ mice (Table 1).

Ectopias receive input from normatopic cortex

Extracellular stimulation of the normatopic cortex surrounding neocortical ectopias elicited both excitatory and inhibitory postsynaptic currents. Evoked EPSCs had both a fast, initial A/K receptor-mediated component and a late, NMDA receptor-mediated component that showed voltage-dependent block at −80 mV. Antidromic responses were rarely observed due to stimulation of the surrounding cortex, and pyramidal cells outside of ectopias were observed to send axon collaterals into ectopias; therefore ectopias receive direct excitatory connections from surrounding normatopic cortex. In the absence of excitatory transmission, IPSCs were elicited by extracellular stimulation of the normatopic cortex surrounding the ectopias. The evoked $GABA_A$ receptor-mediated events were sensitive to $GABA_A$ receptor blockers, BMI and PTX, and exhibited a current-voltage relationship similar to sIPSCs recorded within ectopias. Therefore ectopias also receive direct inhibitory connections from surrounding normatopic cortex.

Although our data suggest that cells within layer I neocortical ectopias receive input, other intracortical connections may be disrupted by the presence of ectopias. Histochemical analysis of ectopia cells injected with biocytin suggests that axon collaterals of cells within ectopias are restricted by the boundaries of the ectopia (Fig. 8*C*), although neurons within ectopias can extend axons along the axon fascicles extending from the base of the malformation (Fig. 8, *B* and *C*). These data suggest that neurons within ectopias may be making aberrant cortico-cortical or subcortical connections. Consistent with this hypothesis, studies using anterograde and retrograde tracers have revealed aberrant thalamo-cortical and cortico-cortical connections (Jenner et al. 2000); however, the functionality of these connections has not yet been elucidated. Based on the considerable amount of evidence suggesting a disruption of normal circuitry, further electrophysiological analysis is needed to determine whether ectopias disrupt normal cortico-cortical and subcortical circuitry.

Comparison to other cortical dysplasias

Heterotopias, such as subcortical band heterotopias (SBH), large collection of ectopic neurons located below the normatopic neocortex in humans, and microgyria, consisting of a four-layered cortex, have been associated with the occurrence of epilepsy in humans (Chugani et al. 1993; Fusco et al. 1992; Lee et al. 1997; Meencke and Janz 1984; Palmini et al. 1991a,b). Animal models of both SBH and microgyria have provided evidence that normatopic neurons, rather than heterotopic neurons, are responsible for initiating epileptiform activity (Chen et al. 2000; Jacobs et al. 1996, 1999; Luhmann and Raabe 1996). In contrast, slices with single ectopias were never found to be epileptogenic either within or outside of the ectopia.

It has been suggested that the hyperexcitability of cells surrounding microgyria in rats is due in part to an imbalance of excitation and inhibition (Jacobs et al. 1996; Luhmann et al. 1998; Prince and Jacobs 1998; Redecker et al. 2000). This imbalance has been characterized by an increase in sIPSC

frequency and amplitude (Prince and Jacobs 1998) and a down regulation of $GABA_A$ receptor subunits (Redecker et al. 2000), as well as an increase in NMDA receptor-mediated input on pyramidal cells (Luhmann et al. 1998) and an increase of NR2B-containing receptors (Defazio and Hablitz 2000) within the epileptogenic cortex of animals with induced microgyria. In contrast, in slices with single ectopias there is no significant difference in the frequency of excitatory or inhibitory events within ectopias as compared with the surrounding normatopic cortex. Epileptiform-like discharges were recorded in two neurons within ectopias in the only slice that contained two adjacent ectopias. This suggests that the presence of multiple ectopias may disrupt the normal balance of inhibition and excitation, thereby creating a hyperexcitable environment. Microgyria and SBHs generally result in much larger cortical disruptions than a single ectopia, indicating that there may be a critical amount of dysplasia necessary to create epileptiform activity.

This work was supported by National Institute of Child Health and Human Development Grant HD-20806 to J. J. LoTurco.

REFERENCES

AGMON A AND CONNORS B. Repetitive burst-firing neurons in the deep layers of mouse somatosensory cortex. *Neurosci Lett* 99: 137–141, 1989.

ARNOLD S, HYMAN B, VAN HOESEN G, AND DAMASIO A. Some cytoarchitectural abnormalities of the entorhinal cortex in schizophrenia. *Arch Gen Psychiatry* 48: 625–632, 1991.

BALOGH S, SHERMAN G, HYDE L, AND DENENBERG V. Effects of neocortical ectopias upon the acquisition and retention of a non-spatial reference memory task in BXSB mice. *Dev Brain Res* 111: 291–293, 1998.

BATTAGLIA G, GRANATA T, FARINA L, D'INCERTI L, FRANCESCHETTI S, AND AVANZINI G. Periventricular nodular heterotopia: epileptogenic findings. *Epilepsia* 38: 1173–1182, 1997.

BERRETTA N AND JONES R. A comparison of spontaneous EPSCs in layer II and layer IV–V neurons of the rat entorhinal cortex in vitro. *J Neurophysiol* 76: 1089–1100, 1996.

BOEHM G, SHERMAN G, HOPLIGHT B, HYDE L, WATERS N, BRADWAY D, GALABURDA A, AND DENENBERG V. Learning and memory in the autoimmune BXSB mouse: effects of neocortical ectopias and environmental enrichment. *Brain Res* 726: 11–22, 1996.

CAULI B, AUDINAT E, LAMBOLEZ ANGULO M, ROPERT N, TSUZUKI K, HESTRIN S, AND ROSSIER J. Molecular and physiological diversity of cortical nonpyramidal cells. *J Neurosci* 17: 3894–3906, 1997.

CAVINESS V JR, EVRARD P, AND LYON G. Radial neuronal assemblies, ectopia and necrosis of developing cortex: a case analysis. *Acta Neuropathol* 41: 67–72, 1978.

CHEN ZF, SCHOTTLER F, BERTRAM E, GALL CM, ANZIVINO MJ, AND LEE KS. Distribution and initiation of seizure activity in a rat brain with subcortical band heterotopia. *Epilepsia* 41: 493–501, 2000.

CHUGANI H, SHEWMON D, SHIELDS W, SANKAR R, COMAIR Y, VINTERS H, AND PEACOCK W. Surgery from intractable infantile spasms: neuroimaging perspectives. *Epilepsia* 34: 764–771, 1993.

CLARK M, SHERMAN G, BIMONTE H, AND FITCH R. Perceptual auditory gap detection deficits in male BXSB mice with cerebrocortical ectopias. *Neuroreport* 11: 693–696, 2000.

DEFAZIO R AND HABLITZ J. Alteration in NMDA receptors in a rat model of cortical dysplasia. *J Neurophysiol* 83: 315–321, 2000.

DENENBERG V, SHERMAN G, SCHROTT L, ROSEN G, AND GALABURDA A. Spatial learning, discrimination learning, paw preference and neocortical ectopias in two autoimmune strains of mice. *Brain Res* 562: 98–104, 1991.

EICHER EM AND LEE BK. The NXSM recominant inbred strains of mice: genetic profile for 58 loci including the Mtv proviral loci. *Genetics* 125: 431–446, 1990.

FLEIDERVISH I, BINSHTOK A, AND GUTNICK M. Functionally distinct NMDA receptors mediate horizontal connectivity within layer 4 of mouse barrel cortex. *Neuron* 21: 1055–1065, 1998.

FRENKEL M, SHERMAN G, BASHAN K, GALABURDA A, AND LOTURCO J. Neocortical ectopias are associated with attenuated neurophysiological responses to rapidly changing auditory stimuli. *Neuroreport* 11: 575–579, 2000.

FUSCO L, BERTINI E, AND VIGEVANO F. Epilepsia partialis continua and neuronal migration anomalies. *Brain Dev* 14: 323–328, 1992.

GALABURDA A, SHERMAN G, ROSEN G, ABOITIZ F, AND GESCHWIND N. Developmental dyslexia: four consecutive cases with cortical anomalies. *Ann Neurol* 18: 222–233, 1985.

GALARRETA M AND HESTRIN S. Properties of $GABA_A$ receptors underlying inhibitory synaptic currents in neocortical pyramidal neurons. *J Neurosci* 17: 7220–7227, 1997.

GUPTA A, WANG Y, AND MARKRAM H. Organizing principles for a diversity of GABAergic interneurons and synapses in the neocortex. *Science* 287: 273–278, 2000.

HABLITZ J AND SUTOR B. Excitatory postsynaptic potentials in rat neocortical neurons in vitro. III. Effects of a quinoxalinedione non-NMDA receptor antagonist. *J Neurophysiol* 64: 1282–1290, 1990.

HANNAN A, SERVOTTE S, KATSNELSON A, SISODIYA S, BLAKEMORE C, SQUIER M, AND MOLNAR Z. Characterization of nodular neuronal heterotopia in children. *Brain* 122: 219–238, 1999.

HENDRY S, SCHWARK H, JONES E, AND YAN J. Numbers and proportions of GABA-immunoreactive neurons in different areas of monkey cerebral cortex. *J Neurosci* 7: 1503–1519, 1987.

HESTRIN S. Different glutamate receptor channels mediate fast excitatory synaptic currents in inhibitory and excitatory cortical neurons. *Neuron* 11: 1083–1091, 1993.

HESTRIN S, NICOLL R, PERKEL D, AND SAH P. Analysis of excitatory synaptic action in pyramidal cells using whole-cell recording from rat hippocampal slices. *J Physiol (Lond)* 422: 203–225, 1990a.

HESTRIN S, SAH P, AND NICOLL R. Mechanisms generating the time course of dual component excitatory synaptic currents recorded in hippocampal slices. *Neuron* 5: 247–253, 1990b.

HUMPHREYS P, KAUFMANN W, AND GALABURDA A. Developmental dyslexia in women: neuropathological findings in three patients. *Ann Neurol* 28: 727–738, 1990.

JACOBS K, GUTNICK M, AND PRINCE D. Hyperexcitability in a model of cortical maldevelopment. *Cereb Cortex* 6: 514–523, 1996.

JACOBS K, HWANG B, AND PRINCE D. Focal epileptogenesis in a rat model of polymicrogyria. *J Neurophysiol* 81: 159–173, 1999.

JENNER A, GALABURDA A, AND SHERMAN G. Connectivity of ectopic neurons in the molecular layer of the somatosensory cortex in autoimmune mice. *Cereb Cortex* 10: 1005–1013, 2000.

KAUFMANN W AND GALABURDA A. Cerebrocortical microdysgenesis in neurologically normal subjects: a histopathologic study. *Neurology* 39: 238–244, 1989.

KAWAGUCHI Y. Groupings of nonpyramidal and pyramidal cells with specific physiological and morphological characteristics in rat frontal cortex. *J Neurophysiol* 69: 416–431, 1993.

KAWAGUCHI Y AND KUBOTA Y. Correlation of physiological subgroupings of nonpyramidal cells with parvalbumin- and $calbindin_{D28k}$-immunoreactivity neurons in layer V of rat frontal cortex. *J Neurophysiol* 70: 987–396, 1993.

KONNERTH A, KELLER B, BALLANYI K, AND YAARI Y. Voltage sensitivity of NMDA-receptor mediated postsynaptic currents. *Exp Brain Res* 81: 209–212, 1990.

LEE K, SCHOTTLER F, COLLINS J, LANZINO G, COUTURE D, RAO A, HIRAMATSU K, GOTO Y, HONG S, CANER H, YAMAMOTO H, CHEN Z, BERTRAM E, BERR S, OMARY R, SCRABLE H, JACKSON T, GOBLE J, AND EISENMAN L. A genetic animal model of human neocortical heterotopia associated with seizures. *J Neurosci* 17: 6236–6242, 1997.

LING D AND BERNARDO L. Restriction of inhibitory circuits contribute to limited recruitment of fast inhibition in rat neocortical pyramidal cells. *J Neurophysiol* 82: 1793–1807, 1999.

LOMBROSO C. Can early postnatal closed head injury induce cortical dysplasia? *Epilepsia* 41: 245–253, 2000.

LOTURCO J, MODY I, AND KRIEGSTEIN A. Differential activation of glutamate receptors by spontaneously released transmitter in slices of neocortex. *Neurosci Lett* 114: 265–271, 1990.

LUHMANN H, KARPUK N, QU M, AND ZILLES K. Characterization of neuronal migration disorders in neocortical structures. II. Intracellular in vitro recordings. *J Neurophysiol* 80: 92–102, 1998.

LUHMANN H AND RAABE K. Characterization of neuronal migration disorders in neocortical structures. I. Expression of epileptiform activity in an animal model. *Epilepsy Res* 26: 67–74, 1996.

MCBRIDE MC AND KEMPER TL. Pathogenesis of four-layered microgyric cortex in man. *Acta Neuropathol* 57: 93–98, 1982.

MCCORMICK D, CONNORS B, LIGHTHALL J, AND PRINCE D. Comparative electrophysiology of pyramidal and sparsely spiny stellate neurons of the neocortex. *J Neurophysiol* 54: 782–806, 1985.

MEENCKE H AND JANZ D. Neuropathological findings in primary generalized epilepsy: a study of eight cases. *Epilepsia* 25: 8–21, 1984.

OTIS T AND MODY I. Modulation of decay kinetics and frequency of $GABA_A$ receptor-mediated spontaneous inhibitory postsynaptic currents in hippocampal neurons. *Neuroscience* 49: 13–32, 1992.

OTIS T, STALEY K, AND MODY I. Perpetual inhibitory activity in mammalian brain slices generated by spontaneous GABA release. *Brain Res* 545: 142–150, 1991.

PALMINI A, ANDERMANN F, AICARDI J, DULAC O, CHAVES F, PONSOT G, PINARD JM, GOUTIERES F, LIVINGSTON J, TAMPIERI D, ANDERMANN E, AND ROBITAILLE Y. Diffuse cortical dysplasia, or the "double cortex" syndrome: the clinical and epileptic spectrum in 10 patients. *Neurology* 41: 1656–1662, 1991a.

PALMINI A, ANDERMANN F, OLIVIER A, TAMPIERI D, AND ROBITAILLE Y. Focal neuronal migration disorders and intractable partial epilepsy: results of surgical treatment. *Ann Neurol* 30: 750–757, 1991b.

PARNAVELAS J, LIEBERMAN A, AND WEBSTER K. Organization of neurons in the visual cortex, area 17, of the rat. *J Anat* 124: 305–322, 1977.

PRINCE D AND JACOBS K. Inhibitory function in two models of chronic epileptogenesis. *Epilepsy Res* 32: 83–92, 1998.

PRINCE D, JACOBS K, SALIN P, HOFFMAN S, AND PARADA I. Chronic focal neocortical epileptogenesis: does disinhibition play a role? *Can J Physiol Pharmacol* 75: 500–507, 1997.

REDECKER C, LUHMANN H, HAGEMANN G, FRITSCHY J-M, AND WITTE O. Differential downregulation of $GABA_A$ receptor subunits in widespread brain regions in the freeze-lesion model of focal cortical malformations. *J Neurosci* 20: 5045–5053, 2000.

ROPERT N, MILES R, AND KORN H. Characteristics of miniature inhibitory postsynaptic currents in CA1 pyramidal neurons of rat hippocampus. *J Physiol* 428: 707–722, 1990.

SALIN P AND PRINCE D. Spontaneous $GABA_A$ receptor-mediated inhibitory currents in adult rat somatosensory cortex. *J Neurophysiol* 75: 1573–1588, 1996.

SCHROTT L, WATERS N, BOEHM G, SHERMAN G, MORRISON L, ROSEN G, BEHAN P, GALABURDA A, AND DENENBERG V. Behavior, cortical ectopias, and autoimmunity in BXSB-Yaa and BXSB-Yaa+ mice. *Brain Behav Immun* 7: 205–223, 1993.

SHERMAN G, MORRISON L, ROSEN G, BEHAN P, AND GALABURDA A. Brain abnormalities in immune defective mice. *Brain Res* 532: 25–33, 1990.

SHERMAN G, STONE L, DENENBERG V, AND BEIER D. A genetic analysis of neocortical ectopias in New Zealand black autoimmune mice. *Neuroreport* 5: 721–724, 1994.

SPENCER D, HUMPHRIES K, MATHIS D, AND LAL H. Behavioral impairments related to cognitive dysfunction in the autoimmune New Zealand black mice. *Behav Neurosci* 100: 353–358, 1986.

SUTOR B AND HABLITZ J. EPSPs in rat neocortical neurons in vitro. I. Electrophysiological evidence for two distinct EPSPs. *J Neurophysiol* 61: 607–620, 1989.

TROTTIER S, EVRARD B, BIRABEN A, AND CHAUVEL P. Altered patterns of catecholaminergic fibers in focal cortical dysplasia in two patients with partial seizures. *Epilepsy Res* 19: 161–179, 1994.

ZHOU F AND HABLITZ J. Metabotropic glutamate receptor enhancement of spontaneous IPSCs in neocortical interneurons. *J Neurophysiol* 78: 2287–2295, 1997.